***Dr. T. Senthilkumar [1], Mrs. H. Vidhya [2], Dr. S. Allirani [3,]**

Dr. T. Vinoth kumar [4]

Design of Hybrid Combination Observer for 4 Phases Switched Reluctance Motor Using FPGA

Journal of Electrical Systems

Abstract: - In recent years, electric drives of SRM have put on more attention seeing as they recommend the possibility of electric drives. However, the SRM has some drawbacks of manifest torque ripple and hearing noises which avoid the use of great performance drives. This paper presents the simulation and experimental review is made for low speed, medium speed, and high speed sensorless speed control of 8/6 Switched Reluctance Motor (SRM) by Field Programmable Gate Array (FPGA) with a combination of Current Sliding Mode Observer (CSMO) and Flux Linkage Sliding Mode Observer (FSMO). Using this combination of CSMO and FSMO the entire speed range are derived. Moreover, Phase Current (PC), Estimation Speed (ES), Actual Speed (AS), and Speed Estimation Error (SEE) of 8/6 SRM are derived from the MATLAB simulation tool. The Experimental setup in 1.0-kilowatt, 8/6, or four phases SRM using FPGA Spartan-6 XC6SLX9-TQG144 is implemented and different speed values like 15 RPM-low speed, 500RPM-Medium speed, and 1500 RPM-High speed are derived and tabulated.

.***Keywords:*** 8/6 Switched Reluctance Motor, CSMO, FSMO, FPGA, ANFIS, PID controller

I INTRODUCTION

Generally, SRM is one of the electric motors which runs through reluctance torque and the working process of the SRM is dependent on the variable reluctance that is motor contained rotor continually tries for aligning with the lowest reluctance lane [1]. Moreover, the formation of the rotary magnetic field is processed with the help of an electronic switching power circuit [2]. Additionally, SRM is considered as a Direct current (DC) motor which imitates the behaviours of the Alternate Current (AC) through switching the DC among the winding of the stator [3]. For controlling the switching operation it needs to use the controller in SRM [4]. Thus the SRM contains many benefits while comparing other electric motors since it has a simple structure, high efficiency, control flexibility, and lower cost [5]. One of the synchronous machines is a reluctance motor that is wounded by the field coil of the DC motor and the rotor contains no magnet or coils on the stator [6]. So the machine is singly excited and double salient.

Frequently it has the gaining efficiency of industrial applications like electric vehicles and wind energy systems because it is a rugged and simple construction, fault tolerance features also has the ability to high-speed operation [7, 8]. Thus the SRM acts as both rotor and stator because it contains salient poles [9]. The main purpose of

[1] [1] Assistant Professor, Department of Electrical and Electronics Engineering, RVS College of Engineering and Technology, Coimbatore-641402, India.

[2] Assistant Professor, Department of Electrical and Electronics Engineering, Sri Ramakrishna Engineering College- 641022, India

[3]Professor, Department of Electrical and Electronics Engineering, Sri Ramakrishna Engineering College- 641022, India

[4] Associate Professor, Department of Electrical and Electronics Engineering, RVS College of Engineering and Technology, Coimbatore-641402, India.

*Corresponding Author, E-mail:texrosen@gmail.com

designed SRM is efficiency in power conversion at high speed and that is comparable through DC motor permanent magnet brushes [10]. As well, SR motor has working with variable principle of reluctance also rotating magnetic field is generated using switching circuit of power electronics [11].

One of the main concepts of the magnetic circuit is changing the air gap between stator and rotor [12]. Thus the rotor and stator are made up of silicon stamping and soft iron. Furthermore, silicon stamping helps minimize hysteresis losses [13]. Consequently, the stators are made up of inward projection also the rotor is outward projection [14]. Improved digital control technology and new control algorithms required for a clean and sustainable source of mechanical energy are steadily making the field of electric drives more complex [15]. The main challenges for modern electric drives are high performance, robust operation and at the same time, having low production costs [16]. In most recent decades the electric drives of SRM have put on more attention seeing as they recommend the possibility of electric drives [17].

To overcome its above drawbacks, the proposed paper describes the combination observer of CSMO and FSMO [18]. The CSMO gives optimum value in high and FSMO gives optimum value in low speed [19]. Both the observer are regulated and synchronized for all low (15 RPM), medium (500 RPM), and high speed (1500 RPM). An experiment is carried out based on four-phase, 8/6 SRM using Spartan-6 XC6SLX9-TQG144 FPGA.

The arrangement of this article is structured as follows: The related work based on SR motor ***is*** detailed in section II and the system model and problem statements are elaborated in section III. Also, process of developed methodology is described in section IV. Finally, the achieved outcomes are mentioned in section V and the conclusion about the developed model is detailed in section VI.

II RELATED WORKS

A few recent literature surveys based on SR motor are detailed below,

FredeBlaabjerg et al [20] developed a novel digital current control technique for avoiding current feedback filters on the SRM current loop. Moreover, symmetrical modulation and synchronized sampling are used to avoid the noise in the sampling filter. Furthermore, FPFA is implemented to enhance and control the steady-state and dynamic current loop. Additionally, developed design increases drive efficiency and minimize switching loss but high cost.

In recent years, micro-hybrid technology is the most attractive method for electric vehicles application because of the energy crisis and pressure. Xiaodong Sun et al [21] proposed a real-time Magnetic Equivalent Circuit (MEC) that contains air gap, iron core, and slot leakage. Moreover, a matrix system is implemented in MEC to speed up the performance. However, the error rate is high.

Paramasivam and Vijayan [22] designed an intelligent speed controller framework using FPGA for controlling the closed-loop speed in SR motor drives. It requires easy mathematical techniques and is mainly based on a discrete control algorithm. Thus the experimental results indicate the correct speed control, operating control speed, setting time, and response time. The designed method attains the best performance to show the operating condition at high speed but with less accuracy.

Nowadays, SRM plays attention and gaining for reducing the power of semiconductor devices. Also, a certain control algorithm is developed to control SRM. Senthilkumar and Wilson [23] proposed a digital controller framework with the help of Digital Signal Processing (DSP) for controlling the speed of SRM. The designed technique is implemented in MATLAB and they are compared with CSMO and FSMO. However, time consumption is more while comparing other techniques.

Divandari et al [24] developed a sensorless SRM drive with a hybrid observer method for estimating the rotor and speed position of SRM. Moreover, designed technique has been implemented in MATLAB tool and the performance of the developed model is compared with FSMO and CSMO. The gained results indicate developed observer and efficiency. Moreover, advantages are high precision and robustness but it has the issue to control the speed.

III SYSTEM MODEL AND PROBLEM DEFINITION

The speed and position of the SRM are estimated using Hybrid Observer (HO) that has illustrated in Fig.1. Additionally, system model of the HO comprises three parts such as the nonlinear technique of SRM, FSMO, and CSMO [25]. Additionally, FSMO and CSMO offer continuous speed and position information to the estimator output with measured amounts of current and voltage. Thus the HO of CSMO and FSMO observe the voltage as well as current sensors for estimating rotor speed and position. It has estimated the rotor speed based on high and low speed and synchronized in the output. Furthermore, a PI controller is used in the algorithm for controlling the SRM speed [26].

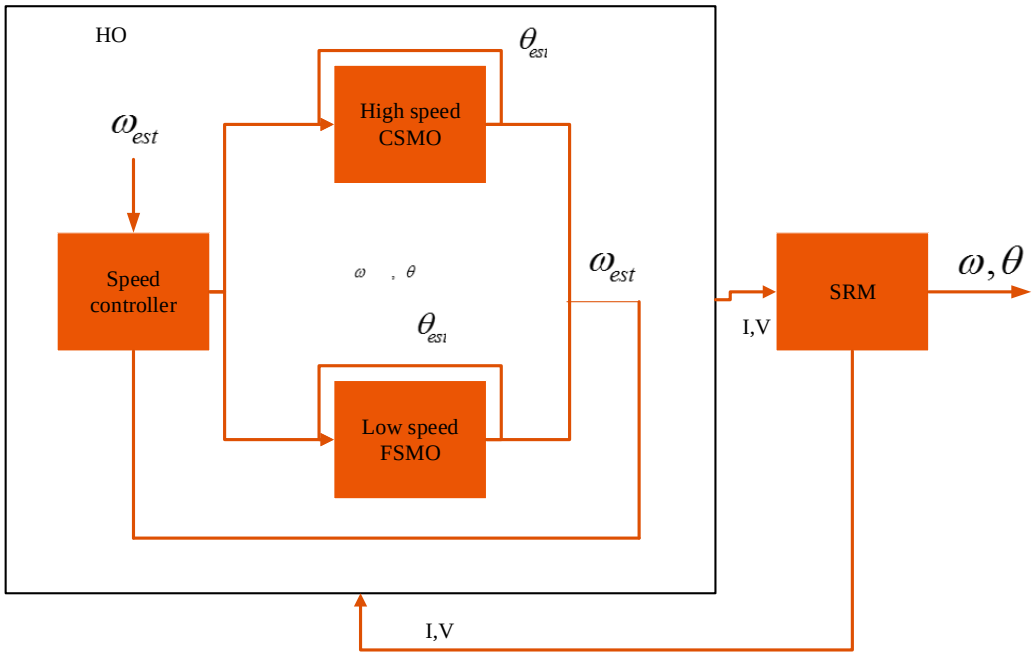

Figure.1. A system model of the hybrid observer in SRM

Additionally, SRM drives are used to identify the torque and flux linkage in all phases which are built using Eqn. (1)

$$T_{eTq} = \sum_{i=0}^{m} T_{que} \tag{1}$$

Let, T_{que} is denoted as torque of ith phase and T_{eTq} is represented as the action of electromagnetic torque.

The motion of the motor mathematical equation is obtained using Eqn. (2)

$$T_{eT} - T_{ld} = I\frac{d\omega}{dt} H\omega \tag{2}$$

Where, T_{ld} is denoted as torque load and I is considered as the moment of inertia of rotor. Moreover, ω is denoted as angular speed and H is called as friction factor with time t.

Consequently, the most problem in SRM drives is less robustness, less accuracy, high time consumption, low performance, and high production cost. There are many techniques are developed to overcome the issues but still have the issues of hearing noise and torque ripple.

IV PROPOSED METHODOLOGY

IV (1) PROPOSED A COMBINATION OBSERVER OF CSMO AND FSMO

A. Mathematical equation of SRM:

The architecture of 8/6 or four phases SRM has illustrated in Fig.1. Here 8 represent stator poles and 6 represent rotor poles. The stator carries winding and rotors have a permanent magnet that tends to align the stator pole axis in the exciting winding [27]. Moreover, the constructional view of 8/6 SRM is shown in Fig.2.

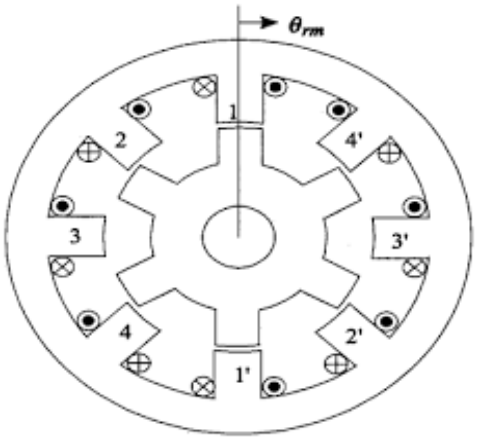

Figure.2 Constructional view of four phases or 8/6 SRM

The mathematical equation of SRM [2] is based on Phase voltage, flux, and current, and the same is derived below,

$$v_k(t) = i_k(t).r_k + \frac{d\phi_k(i_k,\theta)}{dt} \tag{3}$$

With

$$\phi_k = L_k(i_k,\theta).i_k \qquad \text{k =1, 2, 3, 4…..m} \tag{4}$$

$$v_k(t) = i_k(t).r_k + L_k\frac{di_k}{dt} + \frac{\partial\phi_k}{\partial\theta}.\frac{d\theta}{dt}$$

$$v_k(t) = i_k(t).r_k + L_k\frac{di_k}{dt} + \frac{\partial\phi_k}{\partial\theta}.\omega \tag{5}$$

Where, $\frac{d\theta}{dt} = \omega$

The Co-energy of SRM is given by

$$\mathrm{W}_{ce} = \int_0^i \phi\,(\theta,i)di \tag{6}$$

The Torque of the k[th] phase is derived as

$$T_k = \left(\frac{\partial W_{ce}(\theta,i_k)}{\partial\theta}\right)|i_k = Constant \tag{7}$$

$$T_E = \sum_{k=1}^{m} T_k \tag{8}$$

The Mechanical torque of the rotor is:

$$T_{mech} = T_E - B\omega - J\frac{d\omega}{dt} \tag{9}$$

B. Current sliding mode, flux sliding mode, and Combination observer-model equations

Generally, it is the non-linear technique of SRM, CSMO, and FSMO for finding the approximation of rotor position and estimated speed. Additionally, difference among the current actual value and estimated current of non-linear technique of SRM is derived and it is given to the input of CSMO is called Current Sliding Mode Observer [28]. Similarly, the distinction between the real value of flux linkage and flux linkage estimator output is derived and it is given to the input of FSMO is called Flux linkage Sliding Mode Observer. Moreover, block diagram of the combination observer has illustrated in Fig. 3

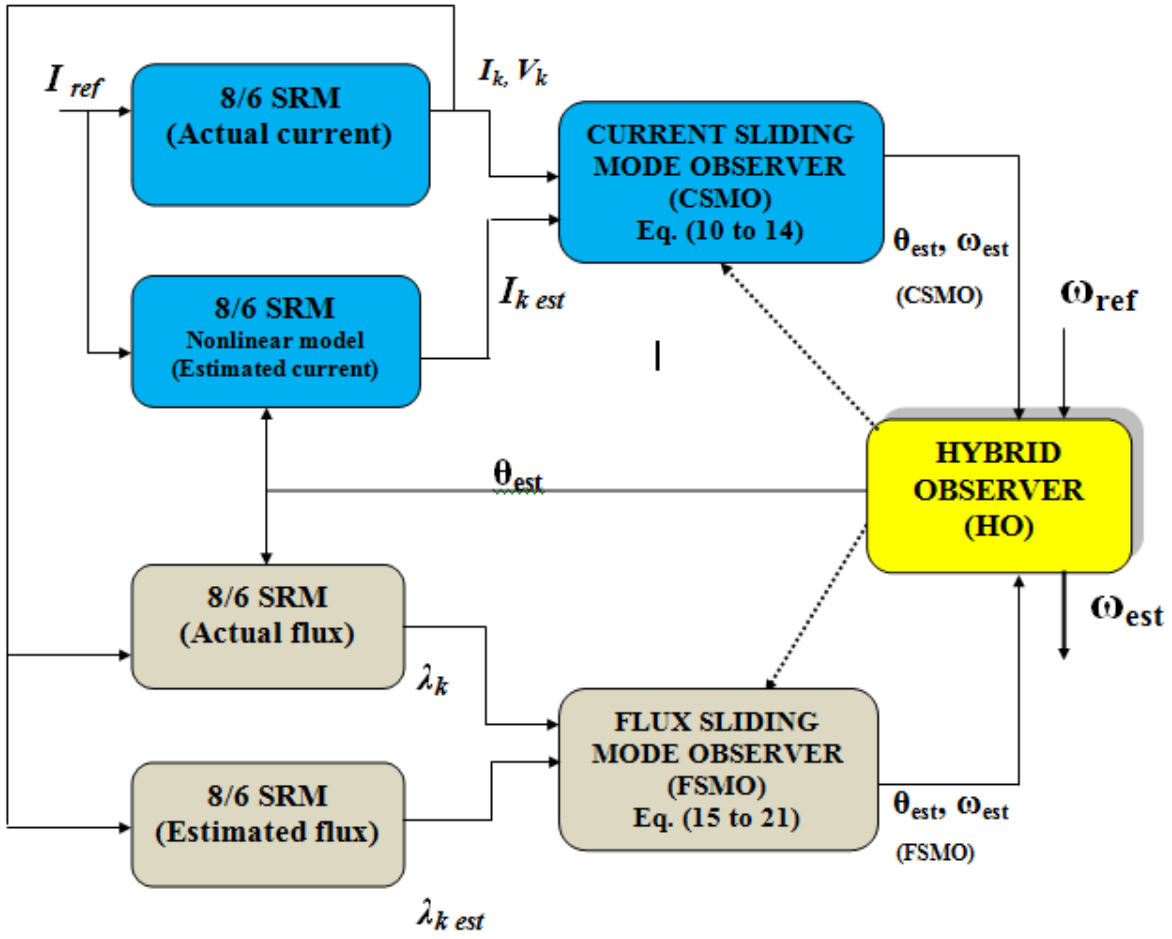

Figure.3 Block diagram of Combination Observer

i) CSMO:

To identify the position of rotor and calculate the speed of SRM, CSMO is constructed based on some measurements. Initially, phase voltage and phase current are measured then simulate nonlinear motor by the same measurements of input voltage [29]. Hereafter, phase current is estimated establish the difference among estimated current as well as actual phase current that are used for estimating rotor speed and position. Furthermore, estimation of CSMO has been developed with help of Equation (8-12) as shown in Fig. 4.

The rotor position and actual speed estimation can be derived as follow

$$X(t) = i_k - i_{kest} \tag{10}$$

Here $X(t)$ is denoted as the difference between the k[th] phase of actual current as well as the estimated current in a CSMO block.

$$X_{cont} = Sign.\sum_{k=1}^{m} X(t) \tag{11}$$

The differential equations of CSMO are:

$$\theta_{est} = \omega_{est} + \beta_{\theta csmo}.X_{cont} \quad (12)$$

with

$$\omega_{est} = T_{est} + \beta_{\omega csmo}.X_{cont} \quad (13)$$

Where, $\beta_{\theta csmo}$&$\beta_{\omega csmo}$ are denoted as CSMO gains.

The estimation error is calculated as

$$e_{\omega} = \omega_{est} - \omega \text{and} e_{\theta} = \theta_{est} - \theta \quad (14)$$

Let,

θ- Rotor position and actual value

ω - Speed and actual value

θ_{est} - Rotor position and estimated value

ω_{est}- Estimated speed

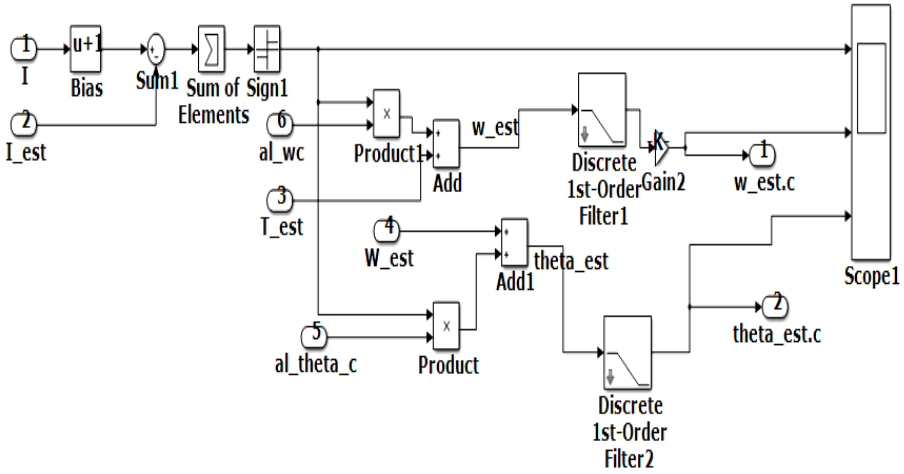

Figure.4 Estimation of CSMO

ii) FSMO:

Generally, FSMO has been determined through difference among actual flux linkage and estimated output of flux linkage [30]. It offers speed information and continuous position based on the measured measures of current and voltage.

Consequently, flux linkage (ψ) of the k[th] phase that is predictable through actual value of each phase current and terminal voltage as follows,

$$\psi_{kest}(t) = \int_{t0}^{t}(V_k(t) - i_k(t).r_k) \quad (15)$$

The k[th] phase flux linkage is,

$$Z(i_k, \theta) = i_k * w_k(\theta) \quad (16)$$

$$\frac{(n-1)*2\pi}{N_{ph}}) \quad (17)$$

$$\psi_k = \psi_s * Z(i_k, \theta) * (1 + \frac{Z(i_k,\theta)^2}{2}) \quad (18)$$

The flux linkage error is given by:

$$e_{\psi} = \sum_{k=1}^{N_{ph}} \frac{dw_k(\theta)}{d\theta} * (\psi_k - \psi_{kest}) | \theta = \theta_{est} \quad (19)$$

The differential equations of FSMO are:

$$\theta_{est} = \omega_{est} + \alpha_{\theta fsmo} * sign(e_\lambda) \tag{20}$$

$$\omega_{est} = \alpha_{\omega fsmo} * sign(e_\lambda) \tag{21}$$

Where, $\alpha_{\theta fsmo}$, and $\alpha_{\omega fsmo}$ are represented as FSMO gains.

The Estimation Block of FSMO has been developed with help of Equation (13-19) as shown in Fig. 5.

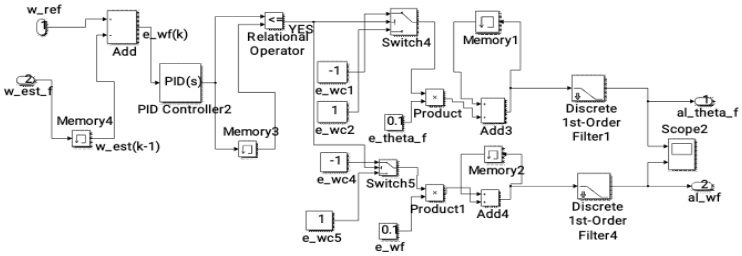

Figure.5 Estimation of FSMO

iii) Combination or Synchronizing of CSMO and FSMO

For finding the rotor position and speed exactly we must need of voltage sensor and a current sensor for each phase [31]. This is the purpose to combine the blocks of FSMO and CSMO for predicting the values of rotor position and speed by using the PID controller. The flow chart of observer selection and synchronizing values is shown in Fig 6.

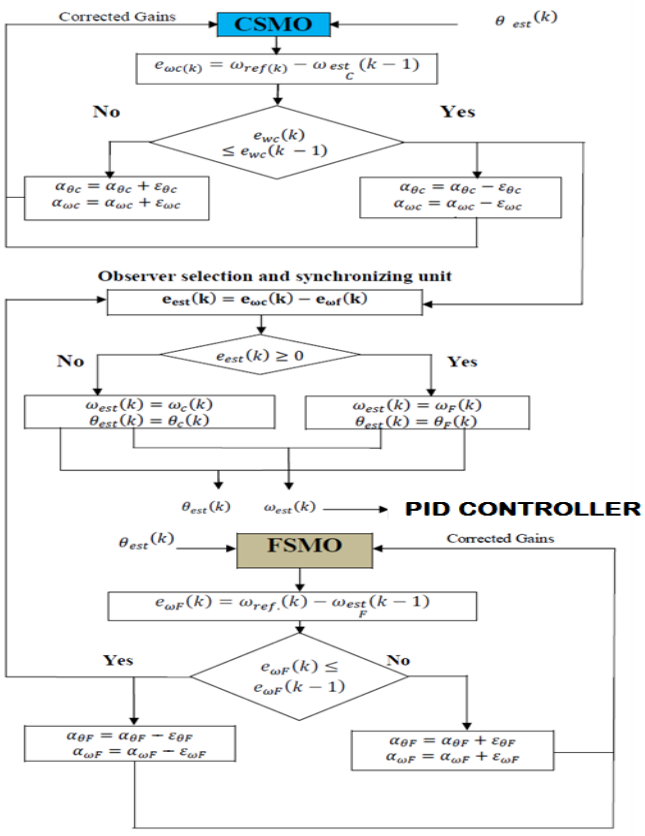

Figure.6 Flow chart of Observer selection and Synchronizing of CSMO and FSMO

The combination observer contains benefit of automatic switching of FSMO and CSMO as well as synchronizing of data between the speeds. i.e. Low to High speed and vice versa.

The value of $\alpha_{\theta c}, \alpha_{\omega c}$ for CSMO and $\alpha_{\theta f}$, $\alpha_{\omega f}$ for FSMO has been synchronized and will be correct with error values.

In addition, the position and speed errors of $e_{\omega}(k), e_{\theta}(k)$resolve by comparing through the previous step of $e_{\omega}(k-1), e_{\theta}(k-1)$ independently in all observer block of FSMO and CSMO also select the superior.

IV (2) PROPOSED ANFIS BASED COMBINATION OBSERVER

The Adaptive Network-based Fuzzy Inference System (ANFIS) become the fuzzy logic structure that contains fuzzy rules and fuzzy sets. Those are determined by the learning procedure based on the principle of artificial neural networks [32]. Moreover, a single fuzzy system explains the information from the training samples but cannot explain the learning information so a combination observer is used in ANFIS to express the ability of learning and flexibility of fuzzy. It controls the speed and identifies the rotor position by loading the fuzzy file which is embedded into the fuzzy block. The experimental waveform results of 1500, 500, and 15 RPM is detailed below,

A. ***At 1500 RPM***

The results of AS, AS, Reference Speed (RS), torque, and SEE for 1500 RPM are shown in Fig.7.

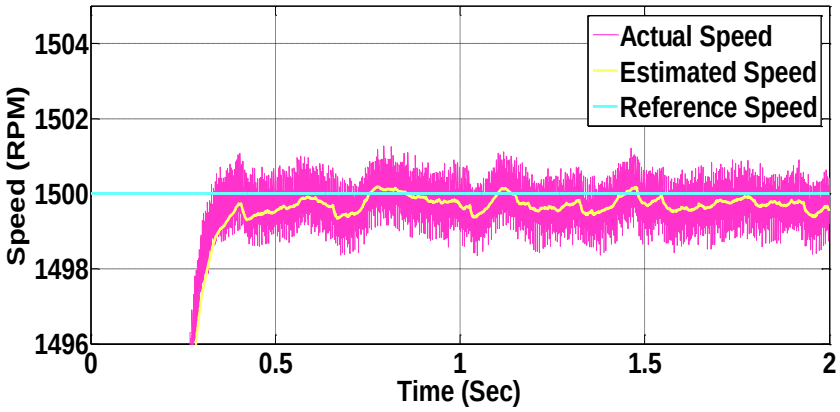

Figure.7 Waveform comparison of Actual, Estimated, and Reference speed at 1500 RPM

The parameters of actual, estimated, and reference speed results are detained in Fig 7, which is observed with ANFIS based combination observer. It shows matches the speed of Actual, Reference, and Estimated Speed with the minimum error of 3 RPM. The results of torque and SEE for 1500 RPM are shown in Fig.8.

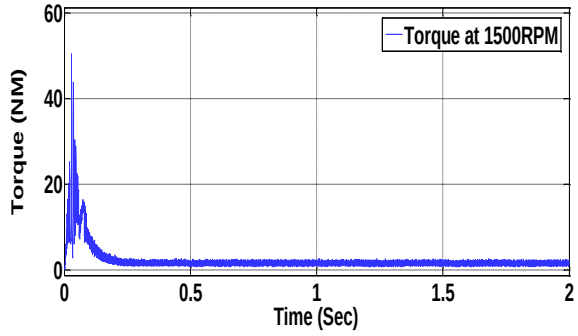

Figure.8 (a) Torque waveform

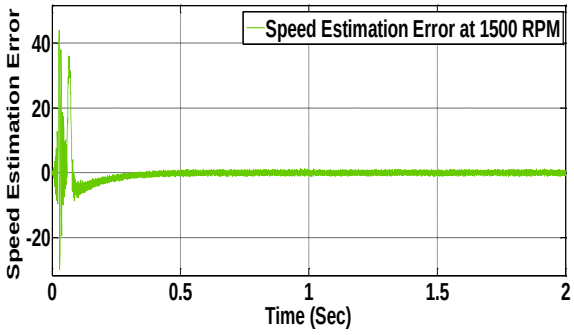

Figure.8 (b) Speed Estimation Error

Figure.8 Torque waveform and SEE at 1500 RPM

In Fig 8 (a), the torque results are observed with ANFIS based Combination Observer. The steady-state operation of 8/6 SRM torque is essentially constant throughout the speed, which gives a better response for high speed (1500 RPM) with low torque ripples. In Fig 8 (b), the SEE with ANFIS based Combination Observer gives the value of 1.8 which the controller output is a low error at high speed.

B. ***At 500 RPM***

The results of actual speed, estimated speed, reference speed, for 500 RPM has illustrated in Fig. 9.

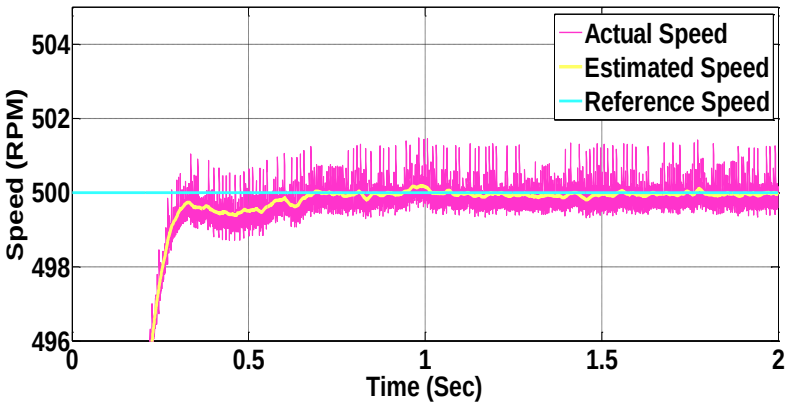

Figure.9 Waveform comparison of AS, ES, and RS at 500 RPM

Fig 9, indicate the matching speed of AS, RS, and ES with the minimum error of 3 RPM. The results of torque and SEE for 500 RPM has exposed in Fig.10.

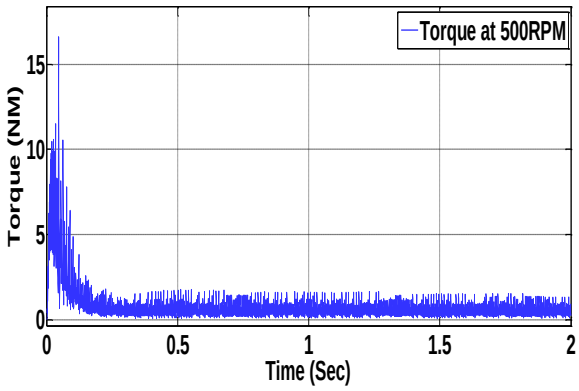

Figure.10 (a) Torque waveform

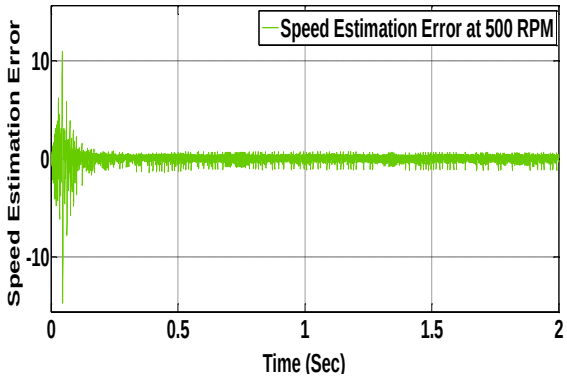

Figure.10 (b) SEE

Fig.10 Torque waveform and SEE at 500 RPM

Fig 10 (a), the torque result is observed with ANFIS based Combination Observer. During starting period of 8/6 SRM torque ripple is moderate which gives the better response in ANFIS at medium speed. The SEE with ANFIS based Combination Observer is shown in fig.10 (b) which gives the value of 0.9 which the controller output is a moderate error at medium speed.

C. At 15 RPM

The results of AS, ES, and RS at 15 RPM are exposed in 11.

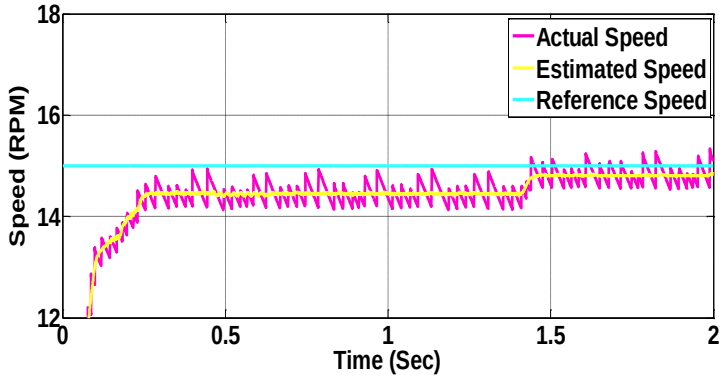

Figure.11 Waveform comparison of Actual, Estimated, and Reference speed at 15 RPM

In Fig 11, the parameters of actual, estimated, and reference speed results are observed with ANFIS based Combination Observer. It shows the speed of Actual, Reference, and Estimated Speed with the minimum error of 2 RPM even at low speed (15 RPM). The results of torque and SEE at 15 RPM are shown in Fig.12.

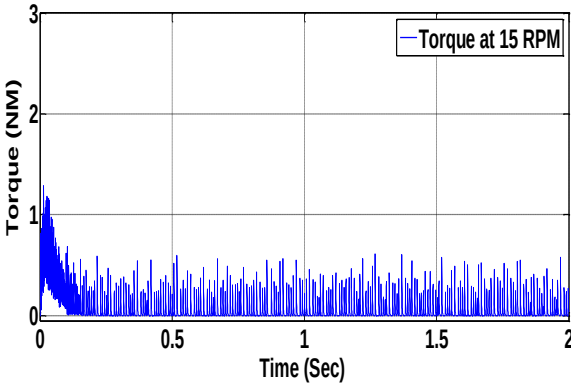

Figure.12 (a) Torque waveform

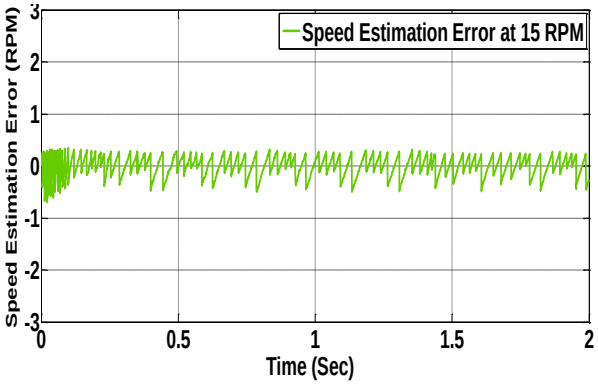

Figure.12 (b) Speed Estimation

Fig.12 Torque waveform and SEE at 15 RPM

In Fig 12 (a), the torque result is observed with ANFIS based Combination Observer. During starting and steady-state period of 8/6 SRM torque ripple is fair which gives the better response of ANFIS at low speed. The SEE of ANFIS based CO has illustrated in Fig. 12 (b) which provide the values of 0.7 which the controller output is moderate error even at low speed.

V. EXPERIMENTAL DISCUSSION AND RESULT

To confirm the Combination observer algorithms, considerable experimental results are accomplished with different speeds 15RPM, 500RPM, and 1500RPM. Moreover, the experimental SRM drive of motor and processor parameters is detailed in Table.1.

Table.1 Experimental SRM drive

Motor Parameters	
Motor Operation Speed	1500 RPM
Rotor Poles	$N_r = 6$
Phases	m = 4
Stator Poles	$N_s = 8$
DC supply Voltage	$V_{dc} = 350V$

Maximum Motor Current	3A
Power Ratings	1HP
Processor Parameters	
FPGA: Controller	Spartan-6 XC6SLX9 in TQG144
Processor speed	20 MHZ
No of ADC input	4 Channels
No of DAC output	4 Channels
Resolution	12 bits
Programmable GPIO Pins	40 pins
ROM	4MB
Analog output range	0 to +5V

The block diagram of sensorless speed control of 8/6 SRM using FPGA through combination observer is shown in Fig. 13. Here we are designed three important segments is controller, asymmetric bridge converter (H-bridge), and its driver circuits.

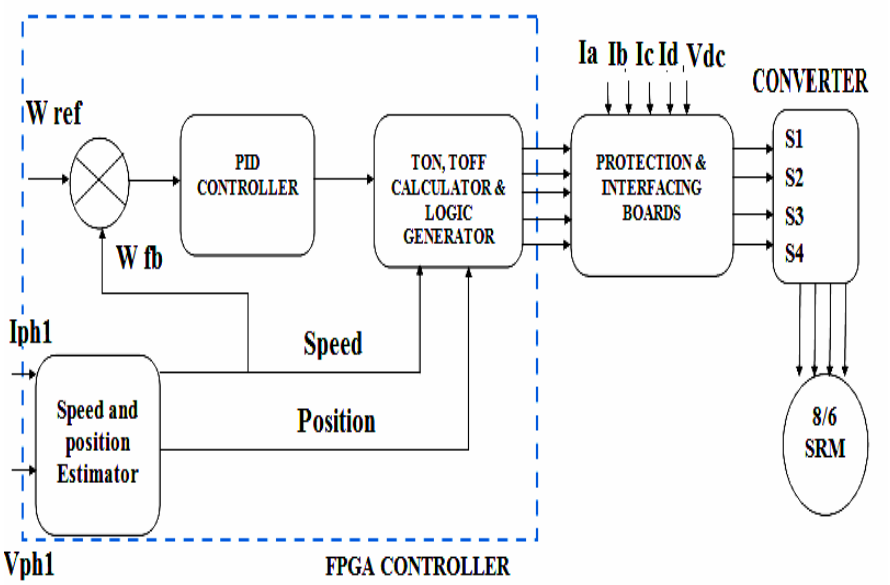

Figure.13 Block diagram of 8/6 SRM drive

For verification of combination observer, the current profile of 1500 RPM, 500 RPM, and 15 RPM is demonstrated with simulation and hardware results.

The torque ripple is minimized or not appeared by using the high switching speed of the FPGA controller [15-18] in the experimental result in DSO.

The sampling period of 1.00 to 1.12 sec is taken in simulation and the hardware results of 10msec are taken for all speed ranges with a load condition of TL=2Nm. Show the waveform of simulation and hardware results as shown in Fig.14 (a) to (f).

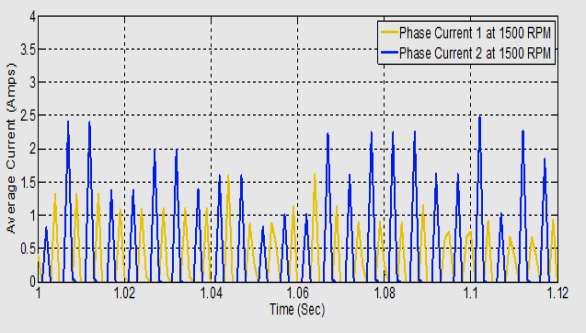

Fig.14 (a) Current profile at 1500 RPM

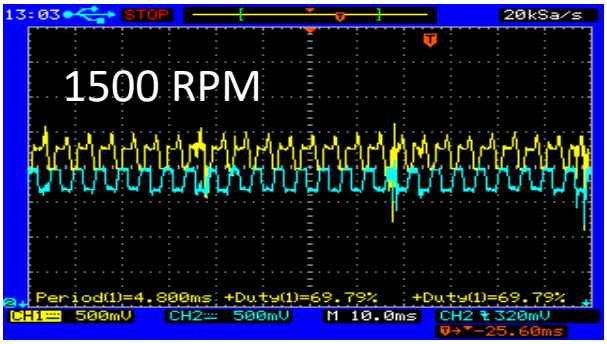

Fig.14 (b) Current profiles at 1500 RPM

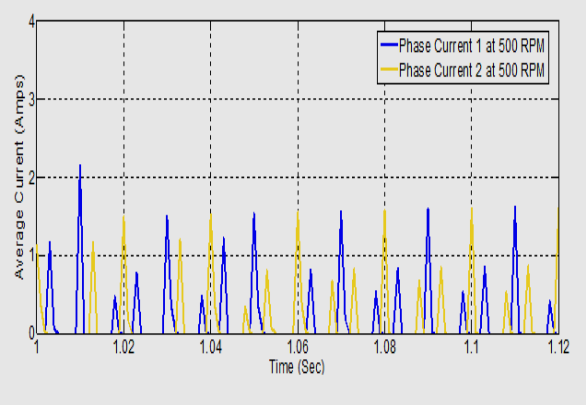

Fig.14 (c) Current profile at 500 RPM

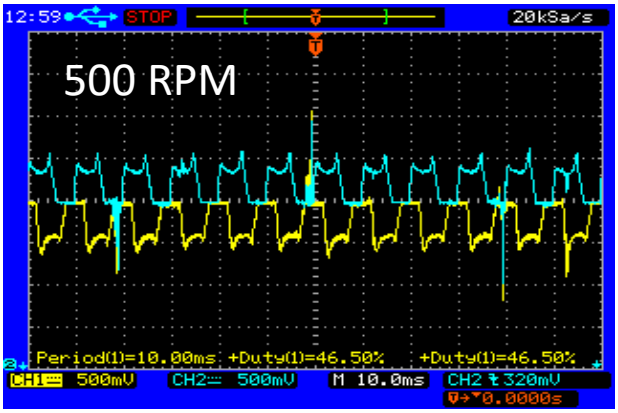

Fig.14 (d) Current profile at 500 RPM

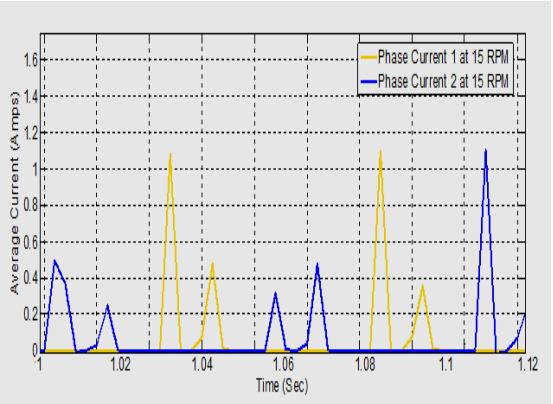

Fig.14 (e) Current profile at 15 RPM

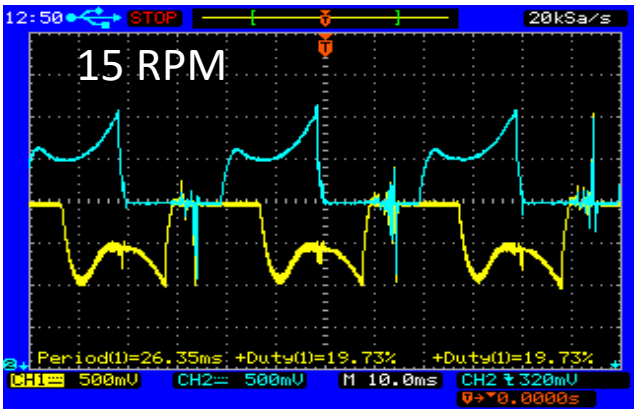

Fig.14 (f) Current profile at 15 RPM

Figure.14 Waveform results of simulation and hardware

From the results values of set speed, torque, and SEE are tabulated in Table.2 using an ANFIS-combination observer.

Table.2

Output Values Using ANFIS Combination Observer

Mode	Set speed (RPM)	Δ Torque (NM)	SEE (RPM)
ANFIS BASED COMBINATION OBSERVER	15	0.3	0.4
	500	0.9	0.9
	1500	1.8	1.1

In the Simulation and Hardware results, the two phases (Phase 1 and Phase 2) are observed for verification purposes and the characteristics or response of the current profile was the same in both. Likewise remaining speed is also observed and verified. The experimental assessment of the four phases 8/6 SRM by inverter driver circuit has illustrated in Fig.15.

Figure.15 Experimental view of 8/6 SRM

The gained output values of with load and without load using ANFIS combination observer is detailed in table.3. It contains the gained results of CSMO, FSMO, and combination observer with 15,500, and1500 RPM.

Table.3

No Load and Load Conditions -Output Values Using ANFIS Combination Observer

WITHOUT LOAD CONDITION					
	Mode	**Set speed (RPM)**	**Average current (Amps)**	**Δ Torque (Nm)**	**SEE (RPM)**
ANFIS	CSMO	15	1.2	2.4	4.0
		500	2	1.8	3.0
		1500	3	1.6	2.6
	FSMO	15	1.0	0.25	0.2
		500	2.5	2.1	2.1
		1500	3.8	2.8	3
		15	**1.2**	**0.4**	**0.3**

	Combination observer	**500**	**2**	**0.9**	**0.9**
		1500	**2.4**	**1.1**	**1.8**
WITH LOAD CONDITION LOAD TORQUE (T_L)=2 Nm					
ANFIS	**Mode**	**Set speed (RPM)**	**Average current (Amps)**	**Δ Torque (Nm)**	**SEE (RPM)**
	Combination observer	**15**	**1.3**	**0.7**	**1**
		500	**2.6**	**1.2**	**1.9**
		1500	**3.5**	**2.1**	**2.2**

Applying load condition in torque, the designed framework set the speed of 15 RPM to attain 1 RPM for SEE, 1.3 Amps for average current, and 0.7 Nm for torque. Moreover, set a speed of 500 RPM to attain 1.9 RPM for SEE, 2.6 Amps for average current, and 1.2 Nm for torque. Additionally, 1500 RPM speed attains 2.2 RPM for SEE, 3.5 Amps for average current, and 2.1 Nm for torque.

Without applying load conditions in torque, the designed framework set the speed of 15 RPM to attain 0.3 RPM for SEE, 1.2 Amps for average current, and 0.4 Nm for torque. Moreover, set a speed of 500 RPM to attain 0.9 RPM for SEE, 2 Amps for average current, and 0.9 Nm for torque. Additionally, 1500 RPM speed attains 1.8 RPM for SEE, 2.4 Amps for average current, and 1.1 Nm for torque.

VI. CONCLUSION

In this work, the CO Algorithm is anticipated by ANFIS. The phase currents also voltages can be easily measured from motor terminals for estimating speed and rotor position. As well, the minimization of torque ripple can be experimental and related from optimization technique mutually. The designed model successfully diminishes the torque ripple in all speeds using ANFIS. Furthermore, simulation outcomes indicate CSMO is appropriate for low and FSMO is appropriate for high speed. But CO attain good performance for low, medium and high speed applications. Consequently, proposed system was planned and implemented using FPGA: Spartan-6 XC6SLX9 in the TQG144 package and its effectiveness in error reduction were demonstrated.

Authors' Contribution *Dr.T.Senthilkumar, Mrs.H.Vidhya, Dr.S.Allirani, Dr.T.Vinothkumar, are discussed and constructed the measures, found their applications, and wrote the paper together.

Compliance with ethical standards

Conflict of interest:

The authors can declare that they have no conflict of interest.

Ethical approval:

This article does not contain any studies with human participants or animals performed by any of the authors.

REFERENCES

[1] T.Senthilkumar and S.U Prabha, "Sensorless Speed Control of 8/6 Switched Reluctance Motor Drive via Hybrid Observer Using ANFIS and Fuzzy-PID," Journal of Electrical Engineering, Vol. 18, Edition 1, No. 48, pp. 435, Feb-March. 2018.

[2] T.J.E Miller, Switched reluctance motors and their control (Magna Physics Publications/Oxford university press, 1993).

[3] V.F.Ray, P.J.Lawrenson, R.M.Davis, J.M. Stephenson, N.N.Fulton, R.J.Blake, High Performance Switched Reluctance Brushless Drivers, IEEE Trans. Ind. Appl., Vol.1A- 22, No.4,1986, pp.722-729.

[4] Y. Cui, X. Yu, H. Fan, J. Fan “The Simulation Study for Switched Reluctance Motor Drives Based on MATLAB6.5”, IEEE Proceeding of Fourth International Conference on Machine Learning and Cybernetics, Guangzhou, PP. 1076-1081, August 2005.

[5] N. K. Dankadai, M. A. Elgendy, S. P. Mcdonald, D. J. Atkinson, and G. Atkinson, "Assessment of Sliding Mode Observer in Sensorless Control of Switched Reluctance Motors," 2019 IEEE 13th International Conference on Power Electronics and Drive Systems (PEDS), Toulouse, France, 2019, pp. 1-6.

[6] S. K. Panda and G. A. J. Amarathunga, “Comparison of two techniques for the closed-loop drive of VR step motors without direct position sensing,” IEEE Trans. Ind. Electron., vol. 38, pp. 95–101, Apr. 1991.

[7] G. Suresh, B. Fahimi, K. M. Rahman, and M. Ehsani, “Inductance based position encoding for sensorless SRM drives,” in Proc. IEEE PESC’99, vol. 2, 1999, pp. 832–837.

[8] D. Reay and B.W.Williams, “Sensorless position detection using neural networks for the control of switched reluctance motors,” in Proc. 1999 IEEE Int. Conf. Control Applications, vol. 2, pp. 1073–1077.

[9] A. Lumsdaine and J. H. Lang, “State observers for variable-reluctance motors,” IEEE Transactions on Industrial Electronics, vol. 37, issue 2, pp. 133–142, April 1990.

[10] J. Cai and Z. Deng, ‘‘Initial rotor position estimation and sensorless control of SRM based on coordinate transformation,’’ IEEE Trans. Instrum. Meas., vol. 64, no. 4, pp. 1004–1018, Apr. 2015.

[11] FeiPeng, Jin Ye, Ali Emadi, Yunkai Huang, "Position Sensorless Control of Switched Reluctance Motor Drives Based on Numerical Method", Industry Applications IEEE Transactions on, vol. 53, no. 3, pp. 2159-2168, 2017.

[12] Design of an Adaptive Flux Observer for Sensorless Switched Reluctance Motors Using Lyapunov Theory, Advances in Electrical and Computer Engineering, ABDELMAKSOUD, H. et al., Advances in Electrical and Computer Engineering 20, 2, p123.

[13] Dong, F., Chen, H., Xu, S. and Cui, S. (2020), "A fault-tolerant sensorless position estimation scheme for switched reluctance motor at low speed", COMPEL - The international journal for computation and mathematics in electrical and electronic engineering, Vol. 39 No. 4, pp. 823-837.

[14] Sivaraju, S. S., and N. Devarajan. "GA based optimal design of three phase squirrel cage induction motor for enhancing performance." International Journal of Advanced Engineering Technology 2.4 (2011): 202-206.

[15] López, I., et al. "Next generation electric drives for HEV/EV propulsion systems: Technology, trends and challenges." Renewable and Sustainable Energy Reviews 114 (2019): 109336.

[16] Orosz, Tamás, et al. "Robust design optimization and emerging technologies for electrical machines: Challenges and open problems." Applied Sciences 10.19 (2020): 6653.

[17] Pereira, Manuel, and RuiEstevesAraújo. "Analysis and design of a speed controller for switched reluctance motor drive." U. Porto Journal of Engineering 5.1 (2019): 46-58.

[18] Blaabjerg, Frede, et al. "Improved digital current control methods in switched reluctance motor drives." IEEE Transactions on power electronics 14.3 (1999): 563-572.

[19] Sun, Xiaodong, et al. "Real-time HIL emulation for a segmented-rotor switched reluctance motor using a new magnetic equivalent circuit." IEEE Transactions on Power Electronics 35.4 (2019): 3841-3849.

[20] Vijayan, S., and S. Paramasivam. "Intelligent speed controller for a Switched Reluctance Motor drive using FPGA." International Journal of Intelligent Systems Technologies and Applications 7.4 (2009): 414-429.

[21] Senthilkumar, T., and A. Wilson Prabhu. "Optimized Speed Control of 8/6 Switched Reluctance Motor Using Digital Signal Processor."Journal of Recent Research in Engineering and Technology ISSN (Online): 2349 – 2252, ISSN (Print):2349 –2260 Volume 5 Issue 1-3 Mar- Dec 2018

[22] Divandari, M., et al. "A novel sensorless SRM drive via hybrid observer of current sliding mode and flux linkage." 2007 IEEE International Electric Machines & Drives Conference. Vol. 1. IEEE, 2007.

[23] Bilgin, Berker, James Weisheng Jiang, and Ali Emadi. "Switched reluctance motor drives: fundamentals to applications." Boca Raton, FL (2018).

[24] Manjula, A., et al. "Performance enhancement of SRM using smart bacterial foraging optimization algorithm based speed and current PID controllers." Computers & Electrical Engineering 95 (2021): 107398.

[25] Wang, Daohan, et al. "Design Consideration of AC Hybrid-Excitation Permanent Magnet Machine with Axial Stator Using Simplified Reluctance Network." IEEE Transactions on Industrial Electronics (2021).

[26] Jarvis, M., S. Schmidt, and A. Malz. "Evaluation of probabilistic photometric redshift estimation approaches for The Rubin Observatory Legacy Survey of Space and Time (LSST)." (2020).

[27] Xu, Y. Z., et al. "Analytical method to optimise turn-on angle and turn-off angle for switched reluctance motor drives." IET Electric Power Applications 6.9 (2012): 593-603.

[28] Ye, Shuaichen, and Xiaoxian Yao. "A modified flux sliding-mode observer for the sensorless control of PMSMs with online stator resistance and inductance estimation." IEEE Transactions on Power Electronics 35.8 (2020): 8652-8662.

[29] Schuhmacher, Klaus, Emanuele Grasso, and Matthias Nienhaus. "Improved rotor position determination for a sensorless star-connected PMSM drive using Direct Flux Control." The Journal of Engineering 2019.17 (2019): 3749-3753.

[30] Ganesan, R., S. Suresh, and S. S. Sivaraju. "ANFIS based multi-sector space vector PWM scheme for sensorless BLDC motor drive." Microprocessors and Microsystems 76 (2020): 103091.